

ILLiad Request Printout

Transaction Number: 330282

Username: OSU Name: Hartley, Charles W

ISSN/ISBN: 0891-2920

NotWantedAfter: 10/20/2007

Accept Non English: Yes

Accept Alternate Edition: No

Request Type: Article -

Resend

Loan Information

LoanAuthor:

LoanTitle:

LoanPublisher:

LoanPlace:

LoanDate:

LoanEdition:

NotWantedAfter: 10/20/2007

Sending in 2 parts

Article Information

PhotoJournalTitle: Archeomaterials.

PhotoJournalVolume: 5

PhotoJournalIssue:

Month:

Year: 1991

Pages: 185-207

Article Author:

Article Title: Vandiver, P.; Ellingson, W.; Robinson, T.; Lobick, J.; and Seguin, F., New Applicati

Citation Information

Cited In: Philadelphia, Pa. ; Archeomaterials, c19

Cited Title:

Cited Date:

Cited Volume:

Cited Pages:

*Scan pictures
in grayscale*

OCLC Information

ILL Number: 34264143

OCLC Number: 14696978

Lending String: *OSU,OSU,INU,INU,INU

Original Loan Author:

Original Loan Title:

Old Journal Title:

Call Number: CC75.7 .A74

Location: ACK Stacks

CGU 128.135.96.233

Notes

9/20/2007 6:00:33 PM System Borrowing Notes; SHARES

New Applications of X-Radiographic Imaging Technologies for Archaeological Ceramics

PAMELA VANDIVER

*Conservation Analytical Laboratory, Smithsonian Institution,
Washington, D.C. 20560*

WILLIAM A. ELLINGSON

*Materials and Components Technology Division, Argonne National
Laboratory, Argonne, Illinois 60439*

THOMAS K. ROBINSON

*Xerox Medical Systems, Xerox Corporation, Pasadena, California
91107*

JOHN J. LOBICK

*Diagnostic Radiology, Rush Presbyterian-St. Luke's Medical Center,
Chicago, Illinois 60612*

FREDRICK H. SÉGUIN*

*Plasma Fusion Center, Massachusetts Institute of Technology,
Cambridge, Massachusetts 02139*

ABSTRACT The ease, availability, and extensive diagnostic capability of radiographic imaging allow details of structure and fabrication to be analyzed for large quantities of sherds and whole pottery vessels so that classification of archaeological ceramics can be done in a more thorough, systematic manner. X-ray imaging modes or sensors that are useful include high-resolution x-ray film, electrostatic plates (xeroradiography), photostimulable phosphors, high resolution computer-aided tomography (CT), and direct digital radiography.

Several factors affect x-ray image content and quality: the experimental limits of detectable density gradients (determined chiefly by the materials present), the dynamic range of the detector, the x-ray energy, and the magnification used in obtaining the image. To demonstrate the simplicity and utility of radiographic imaging as a diagnostic technique, we present several case studies.

INTRODUCTION

Many studies of archaeological ceramics have shown that their structures and method of fabrication can be revealed using modern methods of nondestructive evaluation (NDE) (e.g., Digby 1948; Heinemann 1975; Rye 1977; Alexander and Johnston 1982; Glanzman 1983; Glanzman and Fleming 1985; 1986; Bourriau 1985; Foster 1985; Kingery and Vandiver 1986). NDE data can also be used to help reconstruct the sequence of steps involved in building pottery vessels (e.g., Vandiver 1987; Henrickson 1991) and define technological traditions and technology-transfer when statistically significant numbers of ceramics are imaged (e.g., Vandiver 1987; 1988; 1990; Vandiver and Lacovara 1985-86; Ellingson et al. 1988). Others have used radiography to characterize natural inclusions and temper additions (Braun 1982; Ellingson 1988), but

suitable standards for classifying archaeological ceramics often have not been employed in making identifications (Foster 1985). Despite the information which can be gleaned from radiographic techniques, archaeological reports usually illustrate x-ray images of ceramics only with drawings and photographs, and few radiographic images appear because they are difficult to reproduce.

The use of x-ray imaging to determine variability in ceramic fabrication has now become more common, but it is still limited by the problems of detecting minor density differences between the clay matrix and the heterogeneous materials. To be detected, each type of inclusion or pore must be greater in size than the spatial resolution

* Fredrick Séguin did much of the micro-CT and digital radiography work while employed at American Science and Engineering, Inc., Cambridge, Massachusetts.

limit of the particular x-ray detector being used, must have a sufficient density gradient, and must (except for CT imaging) be sufficiently large compared with the thickness of the sample being imaged. The same information is vital to modern fine ceramics research, and the instruments used in this and other industries can be applied to archaeological ceramics (Ellingson 1988; Mix 1987).

Several commonly available x-ray imaging devices can be used to create inexpensive images of large quantities of vessels and sherds. In order to use the technology most effectively, an understanding of the range of ceramic variables at each stage of processing is necessary, as are well-documented, resource-specific standards which may be established for each set of experiments. We hope that x-ray radiographic NDE will become a routine part of reports on ceramic assemblages and that the data collected from it may be used to create site-, region-, and period-specific databases which may help solve significant archaeological problems.

To begin, we discuss several methods of examination, starting with visual techniques, continuing with other NDE methods not involving radiography, and finishing with five specific radiographic techniques. This is followed by a description of how standards for the inspection of archaeological ceramics can be established through radiographic imaging of objects whose methods of manufacture are known. We then present three detailed case studies illustrating the application of five radiographic imaging techniques to ceramic objects. Finally, we discuss how digital radiographic images can be enhanced by image processing to make it easier to detect specific archaeological ceramic processing features and to help in the publication of x-ray images which can convey greater amounts of information.

METHODS OF EXAMINATION

Visual Examination

Although macroscopic and microscopic visual examinations of external structure and texture are the most basic tools of NDE,

only rarely can they give sufficient detail to reconstruct the sequence of ceramic fabrication. Microscopic examination of residual traces of manufacture is generally more successful for coarse wares than for finer wares where extensive finishing of surfaces has not occurred (Bourriau 1985; Vandiver and Koehler 1986; van As 1984). Although visual examination is less revealing than more sophisticated types of NDE, its use is essential (Rice 1987: 326; Kingery and Vandiver 1986) because it can reveal repetitive patterns of processing and information which are invaluable for determining the appropriate application of more sophisticated techniques.

Other Nonradiographic Inspection Techniques

Many nondestructive imaging methods used frequently in industry cannot successfully provide diagnostic information about the fabrication of ancient ceramics (Vandiver 1985: 49–88). For example, the high porosity in most ancient ceramics prevents the successful application of ultrasound (because of the scatter of elastic waves) and dye penetrants (because of absorption); petrography and scanning electron microscopy are not desirable because only a small part of a vessel can be imaged. Scanning electron microscopy (SEM), petrographic thin section analysis, and texture analysis by x-ray diffraction to detect particle alignment also require extensive, usually destructive sample preparation and cannot be carried out in the field (Vandiver 1985).

Other simple nondestructive imaging methods can be used. For example, rubbings have been used to record relief-decorated surfaces on Jomon ceramics found in Japanese excavations (e.g., Kaneko 1989). This procedure also works well on polished cross sections of porous or coarse tempered earthenware.

Radiographic Imaging Techniques

In the present study, five different x-ray image receptors have been employed in order to compare images and types of information each revealed about fabrication (see Ellingson et al. 1988 for an earlier, prelim-

TABLE 1. Qualitative comparison of the x-ray imaging techniques used in this study

Technique/ receiver	Advantages	Disadvantages	Availability/cost
Ordinary and high-resolution radiography film	High contrast High spatial resolution (2-5 microns) Simple processing Flexible film Film size variable Built-in edge enhancement Wider dynamic range Rapid dry processing No darkroom 126 has lower contrast	Narrow dynamic range Requires dark room wet processing Film image must be digitally scanned Lower spatial resolution (10-20 microns) Plate cassette Limits paper size to 24.5 x 34.5 cm.) No negative 175 has high contrast Requires special laser scanner for read-out Lowest spatial resolution (100 microns) Small plate size 8 x 10 inches	Common in hospitals and museums (can often be carried out on a volunteer basis, or for the cost of technician's time and film)
X-ray source/xeroradiography electrostatic plates			Xeroradiograph 126 available in a few hospitals in major cities; rare in museums; Xeroradiograph 175 new to market and still rare; carried out volunteer or for cost of time and film
X-Radiography/ photostimulable phosphors	Data can be computer enhanced Curved exposures possible Wide dynamic range Nearly linear response Digital radiographic image		Research hospitals only
High resolution micro CT- scanner	Direct view of internal structure Data can be computer enhanced Solid objects can be imaged in sequential cross sections Wide dynamic range	Low spatial resolution (50 microns) Currently limited to 2-inch field Industrial CT systems with imaging fields to 2 meters in diameter with much worse (1 mm.) spatial resolution	Low-resolution (1 mm). CT-scanners are available at research hospitals, and high resolution equipment only at a few research labs
High-resolution direct digital radiography	Can be computer enhanced Widest dynamic range (4000:1)	Low spatial resolution (50 microns) 8 x 8-inch imaging field	Digital systems with resolution at this level available only in research labs

inary study of some of these receptors). The following five imaging media were used: (1) ordinary projection x-radiography with single-sided, high-resolution industrial x-ray film (probably the most common method for imaging ceramics); (2) electrostatic plates, or xeroradiography, in the two modes of the Xerox 126 system (which yields the familiar blue-tone originals) and the Xerox 175 system (which uses black toner and is capable of higher contrast and greater spatial resolution); (3) the recently developed photostimulable phosphor image receptor; (4) a high-resolution x-ray Micro-CT scanner; and (5) a digital radiography instrument. Xeroradiography and high-resolution x-ray film are available in hospitals in most major cities, the others in research hospitals and laboratories (for advantages and disadvantages of these methods, see Table 1). Because film receptors (Nakay-

ama 1953; Todd and Zakia 1969; Kureya et al. 1983; Mix 1987) and xeroradiography (Wolfe 1973; Thourson 1975; Boag 1975; Heinemann 1975; Bokman 1982; Alexander and Johnston 1982; Glanzman and Fleming 1986; Magliano and Boesmi 1988) have been described elsewhere, we will reiterate here only the difference in contrast mechanism.

Xeroradiography is an electrostatic process which produces radiographic images. Values of toner density in the image are not proportional to incident x-ray intensity, as is the case with film, but are related to electrostatic gradients which are caused by variations in x-ray intensity. The incident x-rays passing through the object generate a variation in the density of electric charge on a selenium sulfide plate, and an electrostatic toner distribution in the image is related to the electric field which is caused by gradients in the charge distribution. The

image thus represents not values of density in the imaged object, but gradients in the line-integrated density (which cause gradients in the x-ray intensity at the imaging plate). The net effect is an "edge-enhanced" image in which boundaries and small details are well defined, but from which relative densities of different parts of an object cannot be determined. The specific xeroradiographic systems we used in the following studies are the Xerox 175, which has since been withdrawn from the market, and the Xerox 126.

Digital Imaging Modes

The photostimulable phosphor receptors and the Micro-CT and digital radiography systems (Séguin and Bjorkholm 1988; Séguin et al. 1985) result in digital images—arrays of numbers representing x-ray attenuation—measured at different points in the image plane. Each measurement corresponds to the average over a small but finite area in the plane, called a picture element or pixel. The range of possible gray scale values in each pixel in the image is related to the dynamic range of the digital imaging system, which can be defined as the ratio of the largest to the smallest x-ray intensity level which can be recorded in a single exposure. The spatial resolution of the image is limited by the pixel size, although other characteristics of the x-ray source and detectors can sometimes increase the effective resolution element of the system to a size larger than that of the pixel.

The array of numbers making up a digital image is most commonly displayed on a video monitor using a gray-scale "look-up" table which maps numerical image values to shades of gray. The range of gray scale values in the image is related to the dynamic range of the system. The basic look-up table usually maps the smallest image value to black, the largest image value to white, and intermediate image values to intermediate shades of gray with either a linear or a logarithmic progression. The look-up table can be varied in order to modify the visual contrast of arbitrary parts of the range of image values.

Photostimulable phosphor receptors

Photostimulable phosphor (Sonoda et al. 1983; Takahashi, Kohda, and Miyaha 1984), composed of europium-activated barium fluorohalide compounds, is a relatively new and less available image receptor which can be used in place of film or xeroradiographic plates. Exposure to x-rays excites the photophosphor to a higher energy state and thereby stores the absorbed energy. Subsequent stimulation by visible or infrared light releases the stored energy as luminescent radiation. After the phosphor is exposed to x-rays, the imaging plate is initially sampled by a low-intensity laser which generates a histogram to determine the overall exposure level and dynamic range of the region being examined. The imaging plate is then rescanned by a higher intensity helium-neon laser. The energy stored in the phosphor is released as blue light which is detected by a photomultiplier tube whose sensitivity and amplifier gain have already been adjusted by the preread histogram. This analog information is converted into electrical signals which are digitized, processed, and then recorded on x-ray film by a laser imager. The processing algorithms have been preset to produce automatically a hard copy image which simulates the appearance of a conventional x-ray film, although the data can be post-processed to enhance specific structural features.

The high-resolution phosphor plates, which are reusable, are available in an 8 × 10 inch size. The postprocessed image has a matrix size of 2100 × 2500 pixels, with a spatial resolution of five line pairs per mm. (100 microns). The dynamic range is wide and linear, on the order of 1000:1; thus the plates provide a much wider exposure latitude than film, allowing 10 bits of amplitude resolution in image values.

Storage phosphor technology has a wide latitude as well as the capacity to generate multiple computer-enhanced images from a single radiographic exposure. However, at this time the system's spatial resolution is limited to 100 microns. Until recently, applications of this technology have been in

the medical field, but it can also image objects using radiation which is unsuitable for medical applications, such as particle beams (Kao et al. 1987).

Micro-CT and digital radiography

High-resolution CT systems and digital radiography systems (Séguin et al. 1985; Séguin and Bjorkholm 1988; Séguin 1991) are both based on a specialized 1-dimensional array of x-ray detector elements. The Micro-CT scanner provides images of the cross-sectional structure of objects up to 5 cm. in diameter. Images have 1024×1024 pixels, each 50 microns square. Pixel values correspond to local densities in the cross sections; the images, therefore, give direct information about internal structure without the ambiguities caused by superimposed structures that are common to all projection images. In the case of a ceramic this means that a CT image shows directly what a high-density inclusion looks like. For example, when inclusions are surrounded by pores, it is possible to image even grog, quartz, and feldspar, which have densities similar to the clay matrix (Séguin 1991). The same inclusions would appear in a projection image superimposed on all other inclusions or pores.

The high-resolution digital radiography system used is a research prototype, has better dynamic range than the other projection systems, and offers convenient image processing and a variety of display modes. It provides 4096×4096 images over an 8-inch square imaging field, with 50-micron pixels. The pixel values have 12 bits of amplitude resolution representing 4096 linearly spaced levels of x-ray intensity, giving the widest dynamic range of any of the methods presented here. The spatial resolution of 50 microns and the dynamic range are slightly better than that obtainable with the present photostimulable phosphor images.

An unmodified image (Fig. 1) obtained using high-resolution digital radiography has the overall structural information of film but with poorer spatial resolution. The image can be enhanced through the adjustment of the gray-scale look-up table,



Fig. 1. Abu Hureyra gypsum bowl. High-resolution, digital x-ray projection image of a thick section. The brightness of each pixel is proportional to the log of the x-ray attenuation in passing between the x-ray source and the corresponding location in the image plane; thus brightness is proportional to a line integral of density.

instantaneous switching to the equivalent of the negative image (by inverting the look-up table), and processing methods such as frequency-space filtering. Use of high-pass filtering (Figs. 2, 3) provides information similar to that in xeroradiographic images, but with slightly worse spatial resolution.

DEVELOPING STANDARDS FOR DETERMINING STRUCTURE

Standards for some methods of ceramic manufacture have been established (e.g., Rye 1977; Vandiver 1987), but many are still being defined with new studies which emphasize the sequence of manufacture (which frequently involves several methods). Visual inspection of variations in surface texture, contour, and porosity in well-cleaned edge fractures can be keys in planning how to image a sherd in order to reveal the methods and sequence of manufacture. Likewise, variations in wall thickness,

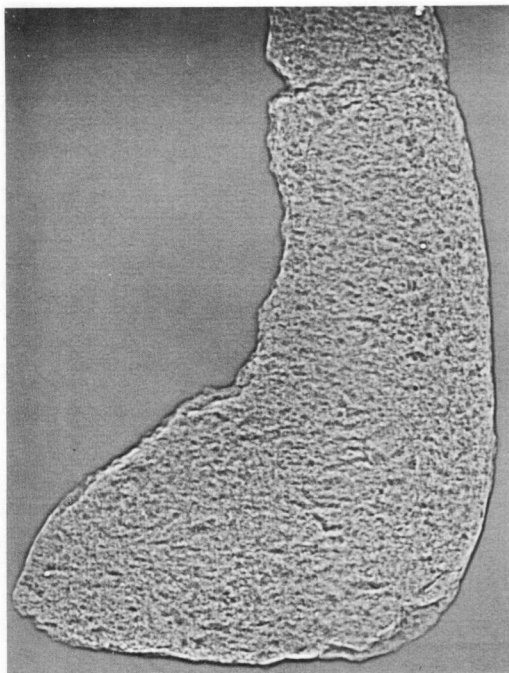


Fig. 2. The image shown in Figure 1 after being mathematically processed with a high-pass filter ("edge enhancement"). Small scale details of all parts of the image are thereby made visible simultaneously.

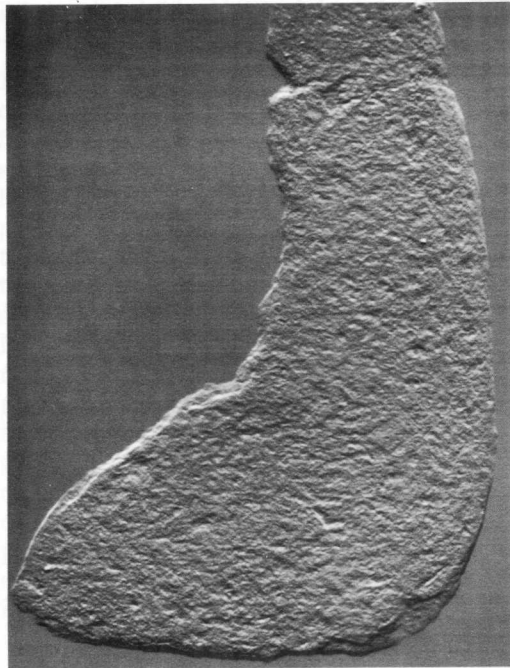


Fig. 3. The image shown in Figure 1 operated on by a directional gradient.

breakage pattern, and shape from one side or part of a vessel to another are also indications of sequence and method of manufacture. The more time spent using a loupe, binocular microscope, or the unaided eye with a glancing or side source of illumination to reveal variations in surface texture, the better one is able to select the "best" samples, anticipate the results of radiography, and plan for the correct placement of the sample in an x-ray imaging apparatus.

In order to develop a standard against which our test samples could be compared, we looked at a typical range of structural variation by imaging ceramic vessels (Fig. 4a) known to have been produced by throwing, coiling, or slab construction techniques.

The positive image (Fig. 4b) of a stoneware pot thrown on an electrically powered fast wheel highlights the variations in wall thickness, incised lines at the neck, and circumferential throwing ridges which appear as horizontal lines. No porosity above the

limit of detection is present in the clay walls because the body was prepared by the modern practice of vacuum extrusion. The negative image (Fig. 4c), on the other hand, accentuates the variations in the thickness of the glaze which appears drippy, thickest at the foot and about one-third the distance up the body from the foot ring. The spherical bubbles correspond to pores in the glaze and are largest where the glaze is thickest, indicating a short time at peak temperature. There are four large inclusions of higher density than the clay body near the largest glaze drip, and another is present on the shoulder above the aforementioned three. These inclusions are not present in the glaze on visual inspection, and therefore are located in the body. A small radial crack in the center of the base is typical of a drying shrinkage problem which occurs when the base dries at a slower rate than the vessel walls; when the base did dry it was held rigidly at the outer edges so only the center yielded.

Next we studied a shiny, black slip-glazed earthenware vessel which was made in the

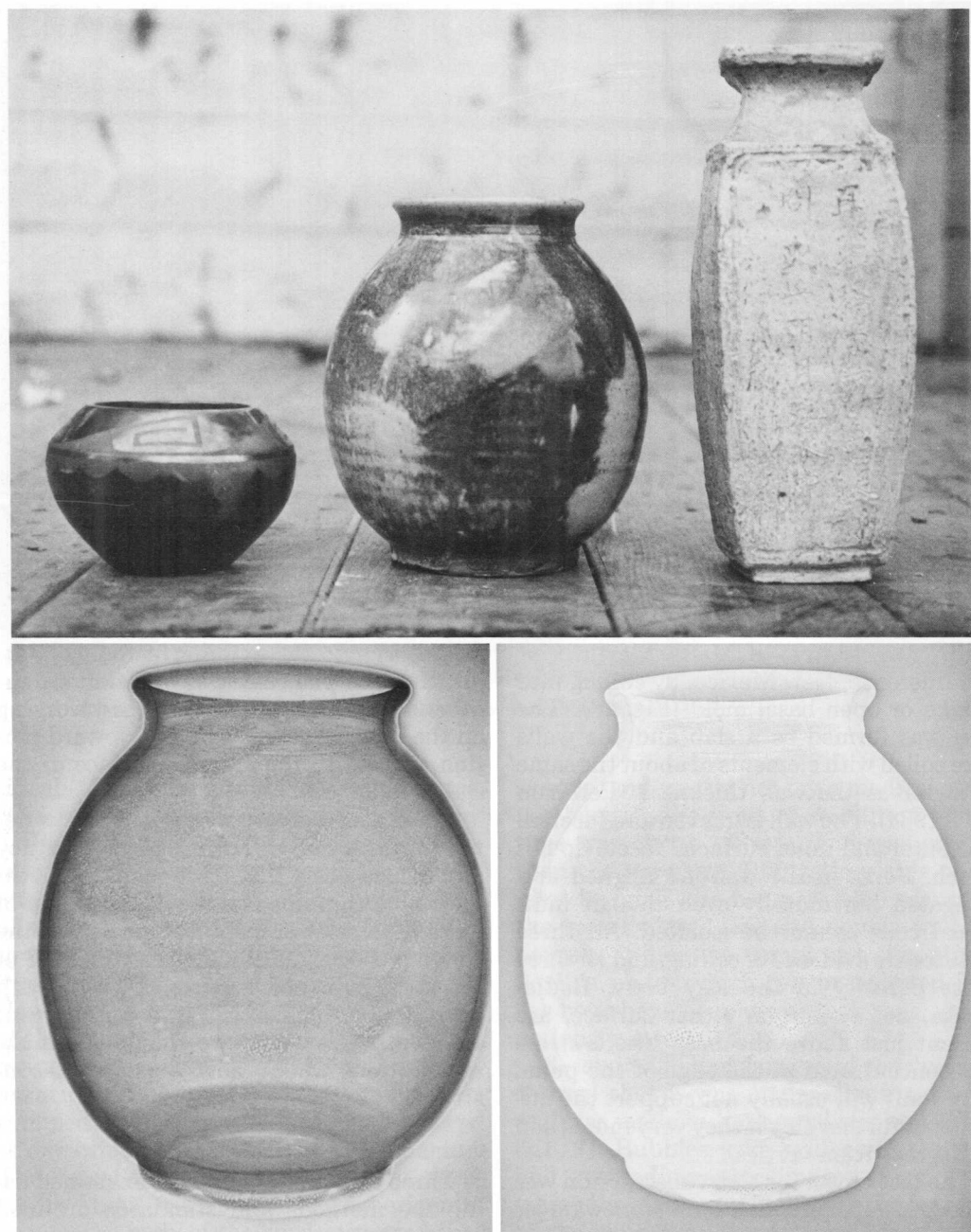


Fig. 4a. Left to right: black slip-glazed earthenware jar from northern New Mexico (San Ildefonso Pueblo), made in the 1940s; red and white glazed stoneware vessel by Vandiver, 1982; Japanese slab-built stoneware vase, ca. 1975. (Collection M.I.T., Department of Materials Science)

Fig. 4b, c. Stoneware vessel. Xeroradiographs using 126 equipment showing slightly different information in positive image of jar (4b) with horizontal throwing ridges, incised lines at neck, rounded pores (white) concentrated where glaze is thick, variations in wall thickness, and crack in base; negative image (4c) showing inclusions with higher (white) and lower (dark) density than the clay matrix. Note that 10 wt% anorthite feldspar was added to the body which is visible as black flecks in the lower left.

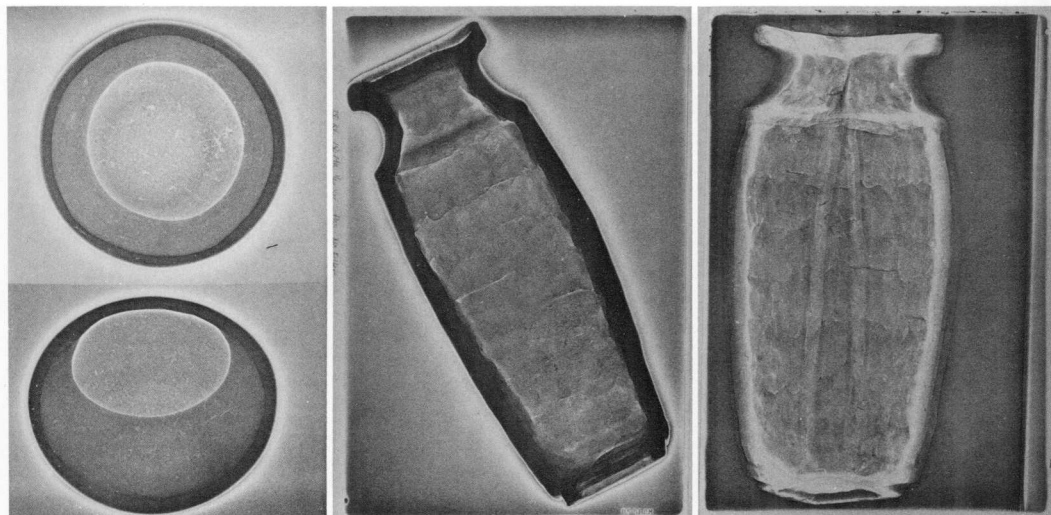


Fig. 4d. San Ildefonso jar. Faceted wall indicates hand building, overall horizontal direction of pores indicates coiling, drying cracks in lower wall indicate use of basal mold or puka by coiling.

Fig. 4e, f. Japanese stoneware vase. Positive and negative xeroradiograph 126 images of irregular horizontal join lines in vase which was built with preformed strips or slabs having joins worked together in downward finger motion on interior and upward motion on exterior

1940s by a relative of Maria Martinez at San Ildefonso, New Mexico, by coiling into a *puka* or open basal mold (Fig. 4d). The base was formed as a slab and the walls were coiled with elements of about the same diameter as the wall thickness (Peterson 1977; 1984). The wall is uneven and faceted. The outer and inner surfacial facets do not match. Pores in the wall are aligned and elongated horizontally even though individual coils cannot be isolated. All three features are evidence of coiling, and all three cause porosity in the clay body. Radial cracks, not visible on either surface, are present just above the base where stress was concentrated at the edge of the *puka*. Clay walls will usually not support the addition of further clay if they vary more than 45 degrees from vertical.

The test object for slab construction was a modern Japanese, slab-built stoneware jar with a square horizontal cross section (Figs. 4e, f; Peterson 1974; Cort 1979; Koyama 1973). The vessel was thought to have been made of four vertical slabs to which the base and circular top were added. However, the pores are elongated horizontally revealing thin strips, and some porosity is present as cracks which in the negative image (Fig. 4f) continue in an upward arc from

the interior to the exterior of the wall, indicating the placement of one slab on another with a consistent downward working on the interior of the wall and upward motion applied to the exterior surface of the slabs at the joints.

These xeroradiographs not only show details of three major forming processes, they also demonstrate that more than one method can be combined in the construction of a single vessel. For instance, the base of the coiled pot consists of slabs and the base of the strip-built pot consists of a slab with an attached ring coil. Thus, it is important to keep in mind that we should not make assumptions about how a pot was constructed.

CASE STUDIES

Three ceramic vessels were examined using the methods and standards outlined above. One was a modern piece and two were archaeological.

Stoneware Bowl

The first sample was a high-footed stoneware bowl (Fig. 5; 13 cm. high × 17 cm. in diameter, Smithsonian Institution No. CAL 1987.344) made in the early 1980s by Fance Franck, a designer for the Manufacture Na-

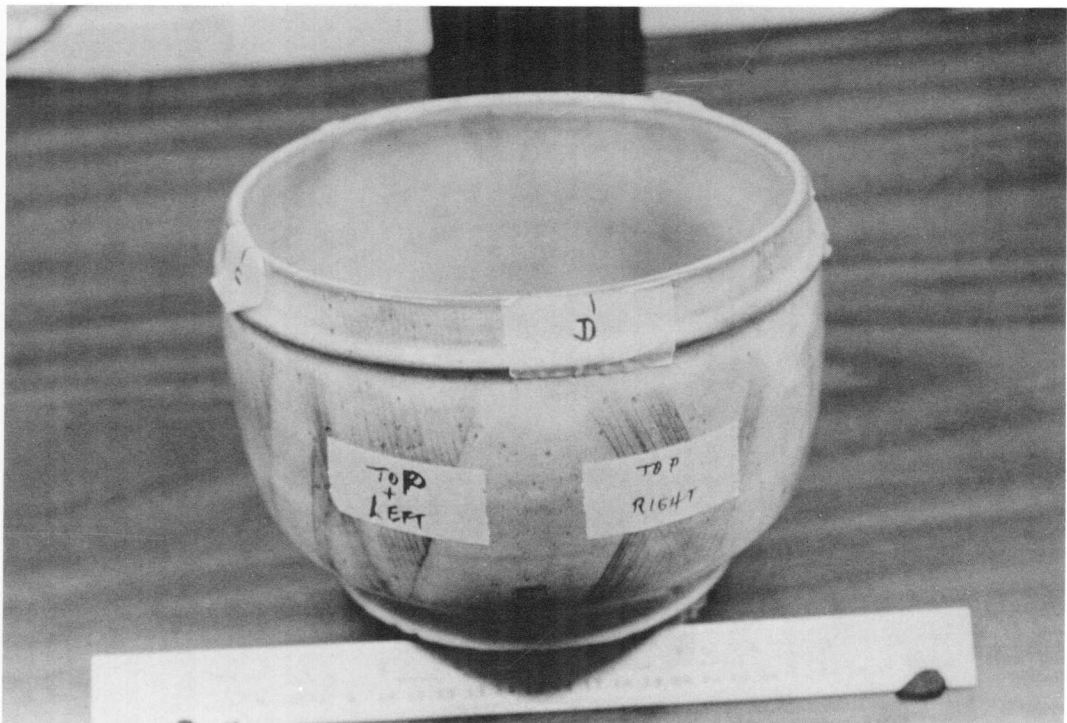


Fig. 5. Contemporary, high-footed stoneware bowl made by Fance Franck, Paris, 1987

tionale des Céramiques de Sèvres, Paris. Rejected because of a radial drying crack in the base, this bowl was donated for study without information on the method or sequence of manufacture, thus providing a blind test. Preliminary visual inspection showed an incised sgraffito decoration made through a white slip with a vitreous, red clay body beneath. The glaze was thicker at the foot and on the ridge below the rim, owing to glaze flow at maximum kiln temperature. The potter's trademark was stamped onto the base of the foot and served as one orientation marker during imaging. The vessel wall was even and thin, measuring about 4 to 5 mm. Two horizontal lines in the body of the bowl suggested that a rib was used during turning or that strips were joined. Visual inspection led to the hypothesis that this bowl could have been thrown or handbuilt.

We did not image this sample using the Micro-CT scanner because the size limitation and geometry of this particular scanner did not permit insertion of so large a

sample, and we did not try a medical scanner because the limit of resolution at the time was about 1.0 mm. and was greater than the pore size. Photostimulable phosphor imaging was not possible because of the vessel's large size and double wall geometry. (Since we completed this study, flexible plates which can be inserted into the bowl have been developed; thus, size is no longer a restriction.)

X-ray imaging of this vessel conclusively showed that it was made of strips of clay and was made in horizontal sections (Figs. 5, 6, 7). Bubbles were evident in the film and xeroradiographic images (Figs. 6, 7) where the glaze was thickest at the foot and at the band near the rim, verifying the visual inspection in which bubbles had been noted in the glaze. In the center of the radiographs where there is virtually no distortion, the larger bubbles in the glaze measured 0.25 to 0.1 mm.; measurement of smaller bubbles requires other techniques. The texture of the clay body was very fine, with less than 5 volume percent of pores

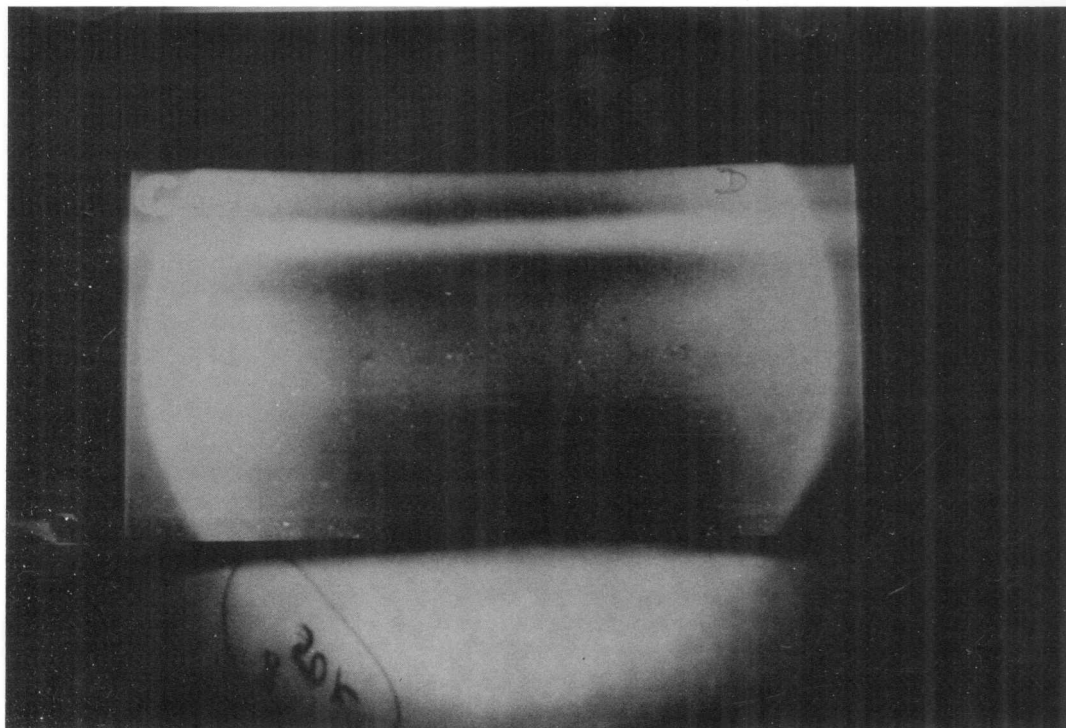


Fig. 6. Stoneware bowl. Single-wall, x-ray image, obtained with industrial Kodak type M vacuum-pack film, showing bubbles in glaze (light), inclusions in the body, and join of horizontal strips used in slab construction

and inclusions above the limit of resolution (Table 2).

We deduced from the film, xeroradiographic images, and optical microscopy that the body was made of a low-shrinkage clay, such as a fireclay, which did not require much added temper. The temper present was at or below 100 microns and possibly of a density too similar to the clay fraction to permit detection.

Lack of symmetry in the placement of one strip above another and the slight deviation of the wall from a constant radius, as viewed from above, corroborated that the vessel was handbuilt rather than thrown. Additional support for this conclusion was the lack of evidence for throwing, such as spiraling ridges, compression furrows, and parallel diagonal-direction pore elongation. A drying or firing crack in the base of the pot showed that it shrank outward toward the ring base and that the foot was added after the wall was at least partly constructed and somewhat dried; it could not, how-

ever, have been added after the pot had been completed because no porosity from the expected differential drying shrinkage is concentrated at the joint of the base and wall.

Franck herself confirmed that the flat base and wall were built first; then the pot was inverted and the foot added with slip and allowed to stiffen, after which the pot was inverted again and the upper wall added. We could not determine where the vertical joints between strips were located, because similar wetnesses of the clay produced no differential shrinkage at the joint. This analysis was also corroborated by Franck, who added that the join was beveled and overlapped for strength and that no slip, but considerable compression, was used at the joint.

Neolithic and Chalcolithic Coarseware Vessels

The second study was of fragmentary West Asiatic Neolithic storage and cooking

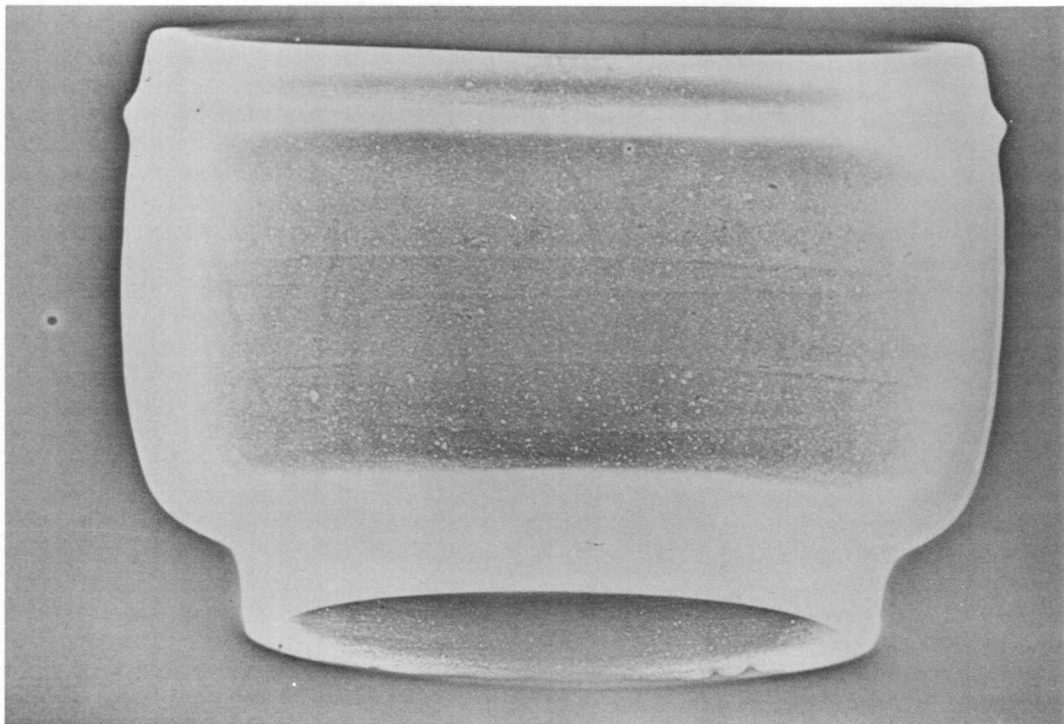


Fig. 7. Stoneware bowl. Double-wall x-ray image, obtained with 126 Xerox imaging plate, showing sensitivity to bubbles in glaze and joining of preformed strips in rings

vessels. The storage vessel was excavated by the University of Pennsylvania Hasanlu expedition at Hajji Firuz, Azerbaijan, Iran (Fig. 8), and dated to the mid-sixth millennium B.C. (Voigt 1983: 152–153, fig. 96c; from Phase A3-E, Operation V); it was cut into sections 1.5 to 2 cm. thick. The other sample, a Chalcolithic cookpot 14 cm. high, from Seh Gabi, was excavated by the Royal Ontario Museum Godin Project and dates to the fourth millennium B.C. (R.O.M. No. 1973 AA21 302; Young and Levine 1974; Vandiver 1987). It had already been determined that they were manufactured by sequential slab construction, although they were initially described as having been handbuilt from either coils or slabs with a slipped surface which was pattern-burnished only where the surface was well preserved. These coarseware ceramics are early examples of a material formed as a fiber-reinforced composite by sequential slab construction. Measurements of the impressions of burned out organic material show

that the original body consisted of about 20 volume percent of chaff and dried grass added as temper. The clay fraction consists of montmorillonite or finely mixed, layered illite-montmorillonite.

Imaging the thick cross sections of the Hajji Firuz vessel fragment using xeroradiographs (both 126 and 175 plates), photostimulable phosphors, and the Micro-CT scanner (Figs. 9–12) shows that the vessel was made in sections from slabs of vegetal-tempered clay which overlapped or butted against one another. The presence of joints, irregular variations in wall thickness, and unevenly faceted surfaces showed the vessel was handbuilt rather than thrown. The more prominent joints indicate that the vessel was built in sections, each consisting of several slabs. Each section represents the result of one work session, with partial drying between each session. The vegetal temper in this fiber-reinforced composite helped identify joints. The fibrous plant temper bent around at the joints, giving a charac-

TABLE 2. Densities of pores and inclusions relative to fired clay bodies

	Specific gravity e.g., earth- enware	Relative specific gravity/ e.g., inclu- sion
Common base materials		
Fired Earthenware	2.5	1.0
Stoneware and Porcelain	2.6	0.96
Imaged		
Air	1.0	2.5
Halite*	2.16	1.16
Sometimes imaged		
Gibbsite*	2.3–2.4	1.06–1.04
Cristobalite	2.30–2.32	1.06–1.08
Gypsum*	2.32	1.08
Not imaged		
Earthenware Clay Grog*	2.6	0.96
Kaolinite*	2.6–2.63	0.96–0.95
Quartz*	2.65	0.94
Feldspars		
K-spars microcline	2.54–2.57	0.98–0.97
Orthoclase*	2.57	0.97
Sanidine	2.56–2.62	0.97
Albite*	2.62	0.95
Sometimes imaged		
Feldspars		
Plagioclase	2.62–2.76	0.95–0.91
Anorthite*	2.76	0.91
Chlorite	2.6–3.3	0.96–0.76
Talc*	2.7–2.8	0.93–0.89
Calcite*	2.71	0.92
Imaged		
Mica biotite*	2.8–3.2	0.89–0.78
Muscovite (sericite)*	2.76–2.88	0.91–0.87
Wollastonite*	2.8–2.9	0.89–0.86
Anhydrite*	2.89–2.98	0.87–0.84
Aragonite	2.95	0.85
Apatite*	3.15–3.2	0.79–0.78
Olivine	3.27–4.37	0.76–0.57
Rutile	4.18–4.25	0.60–0.59
Fayalite	4.39	0.57
Zircon	4.68	0.53
Ilmenite	4.7	0.53
Hematite	4.8–5.3	0.52–0.47
Magnetite*	5.18	0.48

Inclusions of those materials marked * were ground and sieved to sizes of 0.1–1.0 mm. and mixed with a low-shrinkage, iron-bearing earthenware clay (A.P. Green Red Art) of 5 mm. thickness, such that the average maximum particle size was 10% of the thickness of the clay cross section. Tiles 3 × 12 mm. were fired to 900°C prior to imaging.

teristic pattern at butt and bevel joints. The chaff has two functions: to strengthen and stiffen the wall during construction, and to prevent shrinkage during drying.

The photostimulable phosphor process has a greater dynamic range but poorer resolution than xeroradiography (Figs. 9, 10); the Xerox 175 process has good contrast

but lower range (Fig. 11). The Micro-CT image (Fig. 12) shows what the internal structure on a cross section through the sample looks like. Elongated pores (dark areas) are clearly distinguishable from the equiaxed inclusions (light spots). A vertical joint interface is present one third of the distance from the left surface.

When the high-resolution film x-radiography and 126 xeroradiography are compared (Figs. 13, 14), the smaller dynamic range and better edge enhancement of the electrostatic process become evident. The low contrast of the blue xeroradiography 126 image makes it difficult to reproduce in a black and white publication. Printing an x-ray film image to illustrate construction processes is also difficult because the dynamic range is smaller and the contrast is much wider than in printed media, yielding generally poor results. The thick base is underexposed and the rim is overexposed, although in viewing the original film, the eye can compensate for the variation.

Pre-pottery Neolithic Plaster

The third sample was a fragment of a Pre-pottery Neolithic plaster bowl from Abu Hureyra, Syria (Fig. 15), which dates to about 6400 B.C. (Moore, in preparation). This and similar bowls known from contemporaneous sites are referred to as *vaiselle blanche* or white ware. Earlier work using x-ray diffraction and scanning electron microscopy of similar pieces has identified the vessels as plasters made from calcined gypsum (calcium sulfate). The precursor of pottery in West Asia was plaster (Gourdin and Kingery 1975; Kingery, Vandiver, and Prickett 1988), indicating that kilns and firing technology were developed before the invention of clay-based pottery. Establishing details of the manufacture of vessels from Abu Hureyra enables us to determine whether the methods of manufacture employed for early clay-based coarseware pottery, such as the sample from Hajji Firuz and vessels from other West Asiatic sites, were indeed those of the earlier plaster technology.

The x-ray receivers did not demonstrate manufacturing evidence for the Neolithic plaster bowl fragment, even though some macrostructural evidence of joints is visible

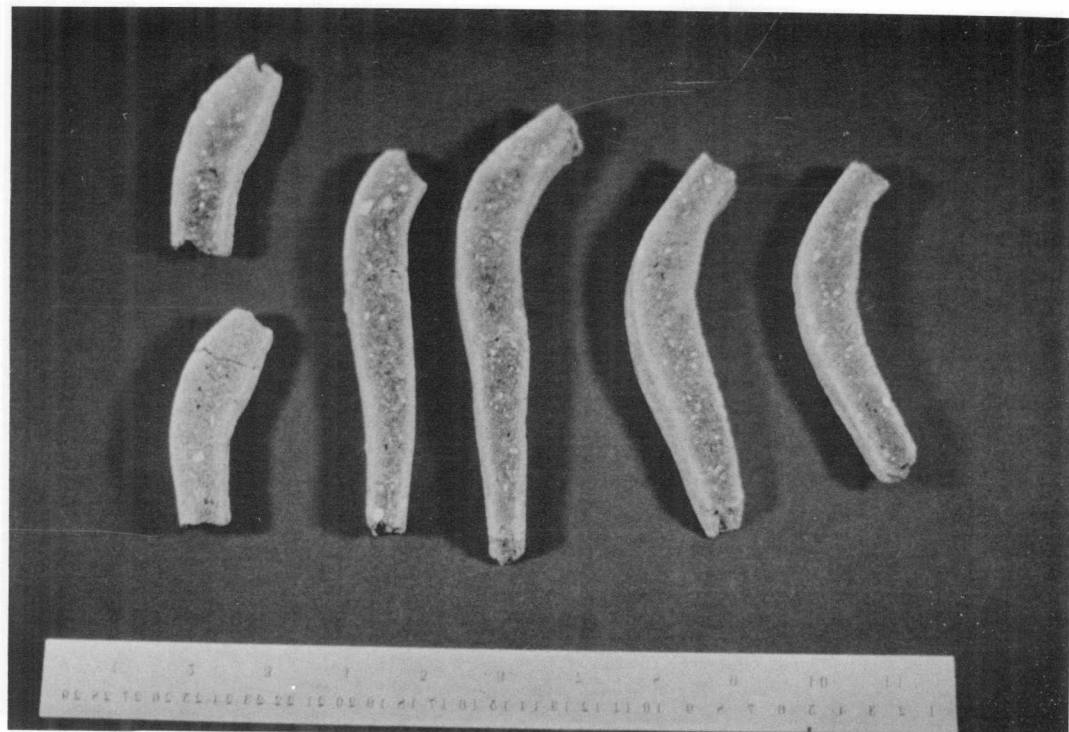


Fig. 8. Fragments (thick section slices) of a storage vessel from Hajji Firuz, Azerbaijan, Iran, ca. 5500 B.C.

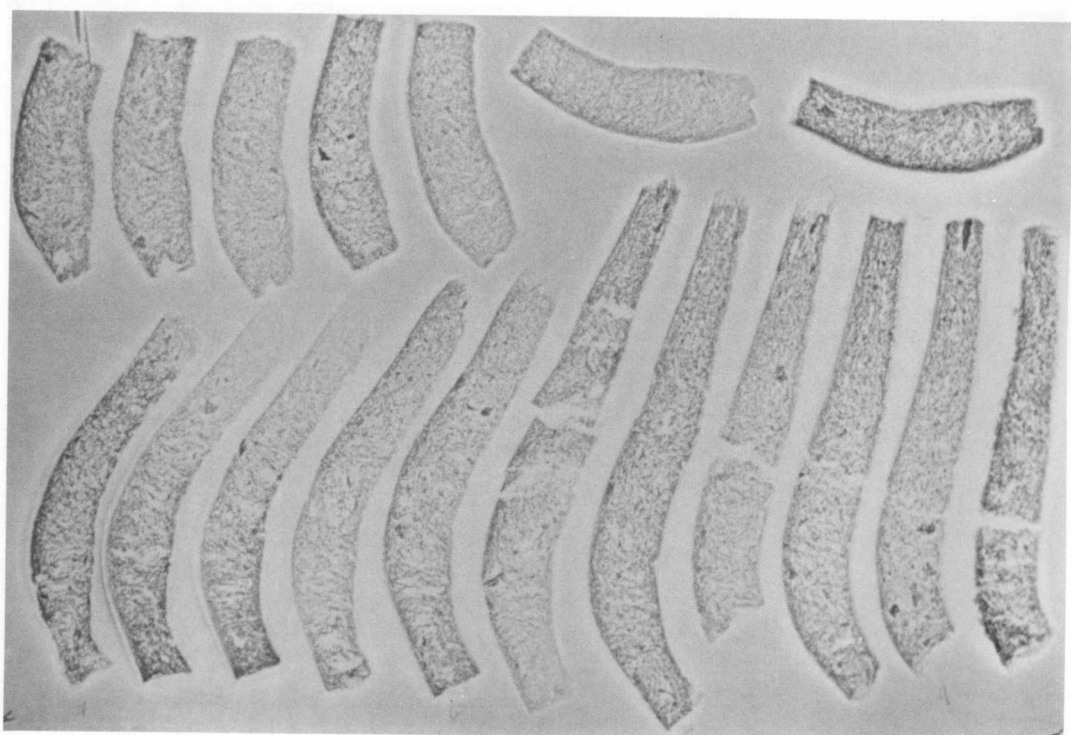


Fig. 9. Hajji Firuz storage vessel. X-ray image of thick-section fragments obtained with Xerox 126 imaging plates

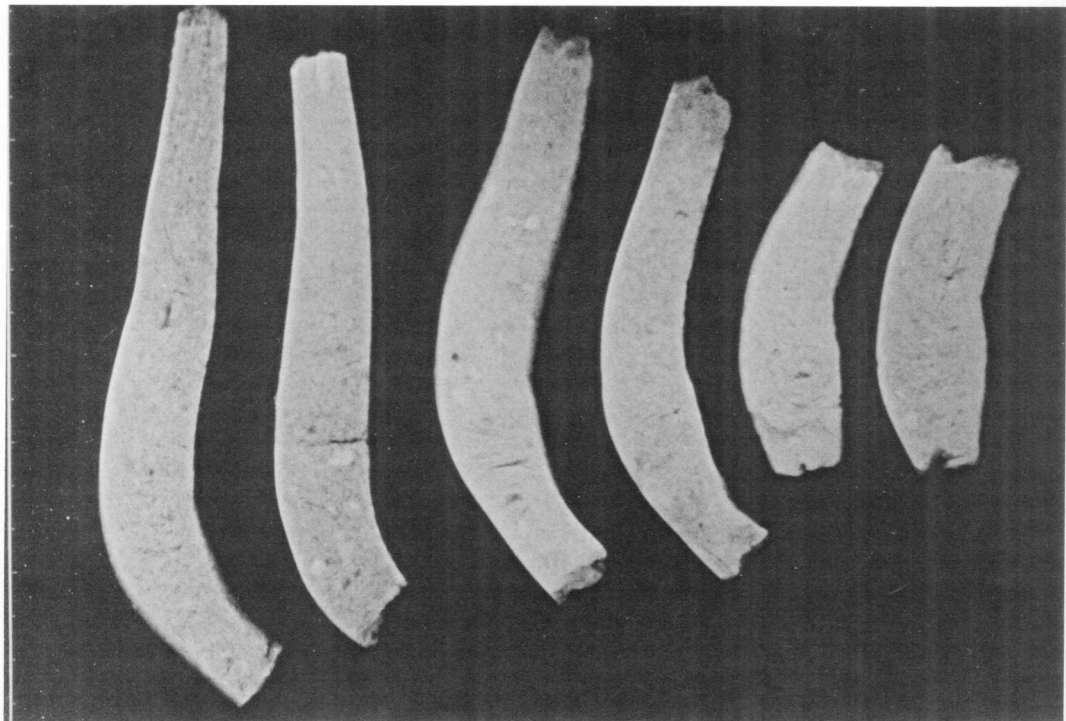


Fig. 10. Hajji Firuz storage vessel. X-ray image of thick section fragments obtained with photostimulable phosphors as the x-ray image receptor

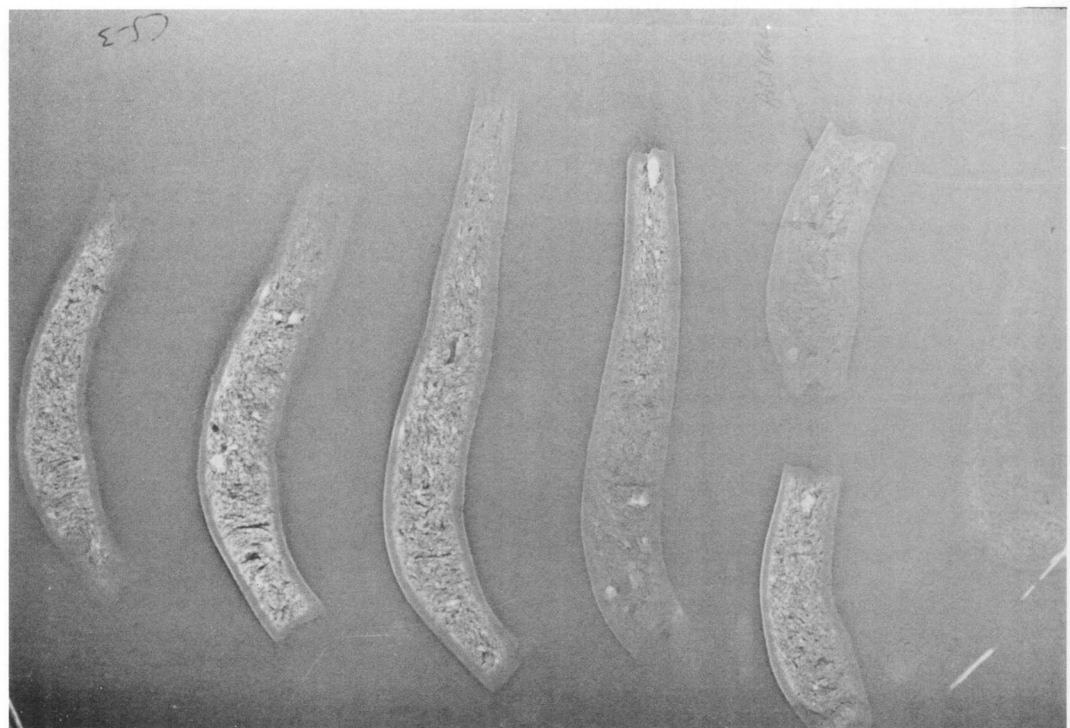


Fig. 11. Hajji Firuz storage vessel. X-ray image of thick section pieces obtained with Xerox 175 imaging plates

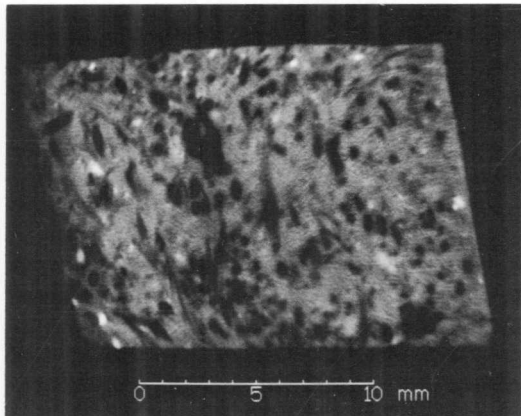


Fig. 12. Hajji Firuz storage vessel. Micro-CT image of a slice through a thick section. Elongated pores from fiber burnout and low density inclusions are black, and high density inclusions are white.

on the surfaces. Contact x-ray images obtained with industrial single emulsion film (Fig. 16), a 126 Xerox plate (Fig. 17), and photostimulable phosphors (Fig. 18) show

the variation in dynamic range of each image receiver; the characteristic low dynamic range of x-ray film is clearly evident. A Micro-CT image of a small 35×15 mm. slice taken from the plaster bowl fragment shows pores (black) and inclusions (white) (Fig. 19). There is no clear indication of a joint, although the pores are concentrated near the irregular, outer vessel surface (lower edge) and in a diagonal starting about two-thirds of the distance to the right and proceeding to the upper left, which is the position of the joint indicated by a step joint on the surface. A projection image of the Abu Hureyra fragment was taken with the 50-micron-resolution digital radiography system (Fig. 1; see Figs. 2, 3 for postprocessed versions). When a joint is present, as is visually indicated by the overlapping flange and continuous horizontal crack at the surface, then several interpretations are possible: the interface has no characteristic structure, the structure is not visible at the

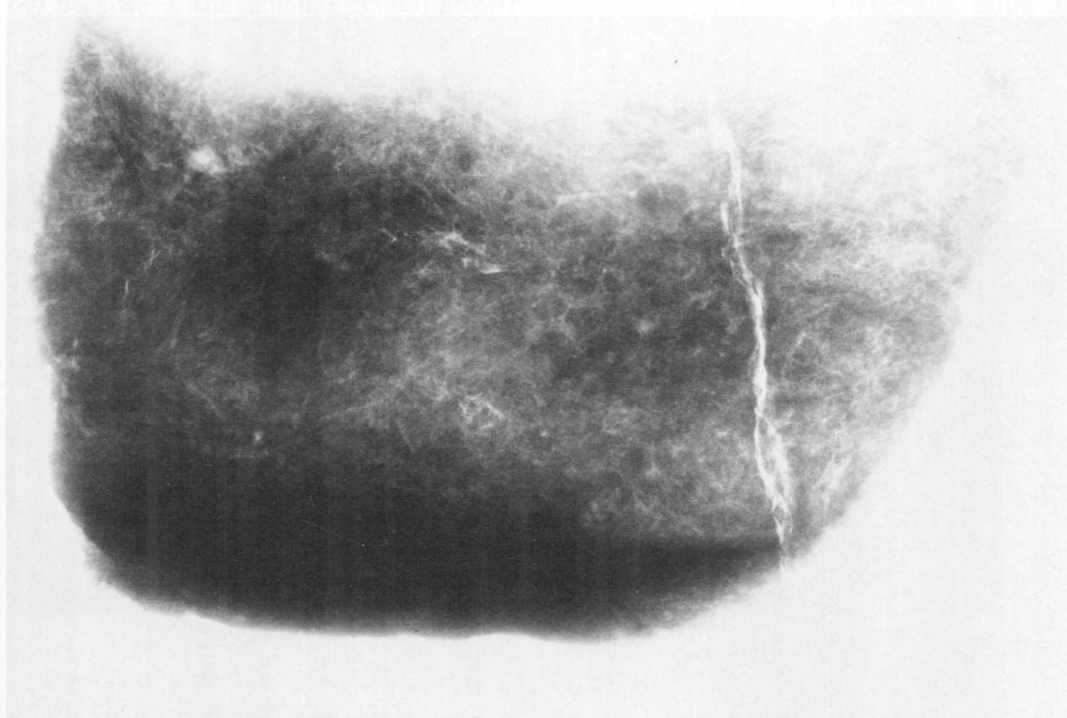


Fig. 13. X-ray image of a Chalcolithic cookpot from Seh Gabi, Iran, made by sequential slab construction with staggered, patted out handfuls of chaff- and straw-tempered clay. Section join occurs at 2/3 height. (Royal Ontario Museum, No. 1973 AA21 302)

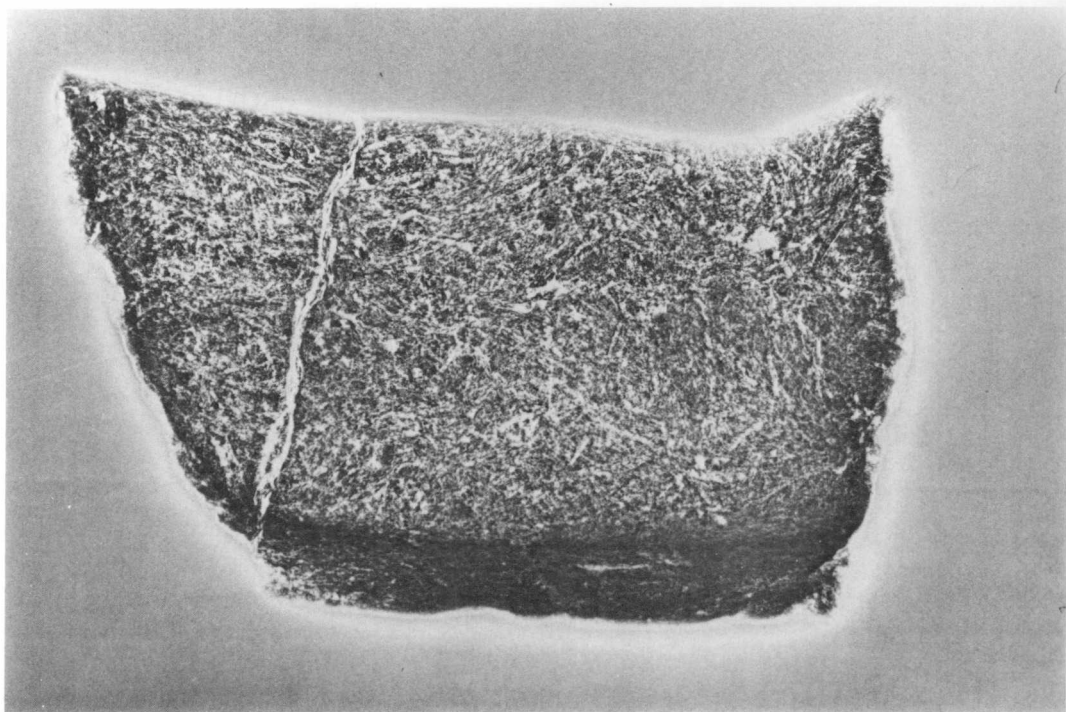


Fig. 14. Sherd in Fig. 13 imaged with a 126 Xerox plate

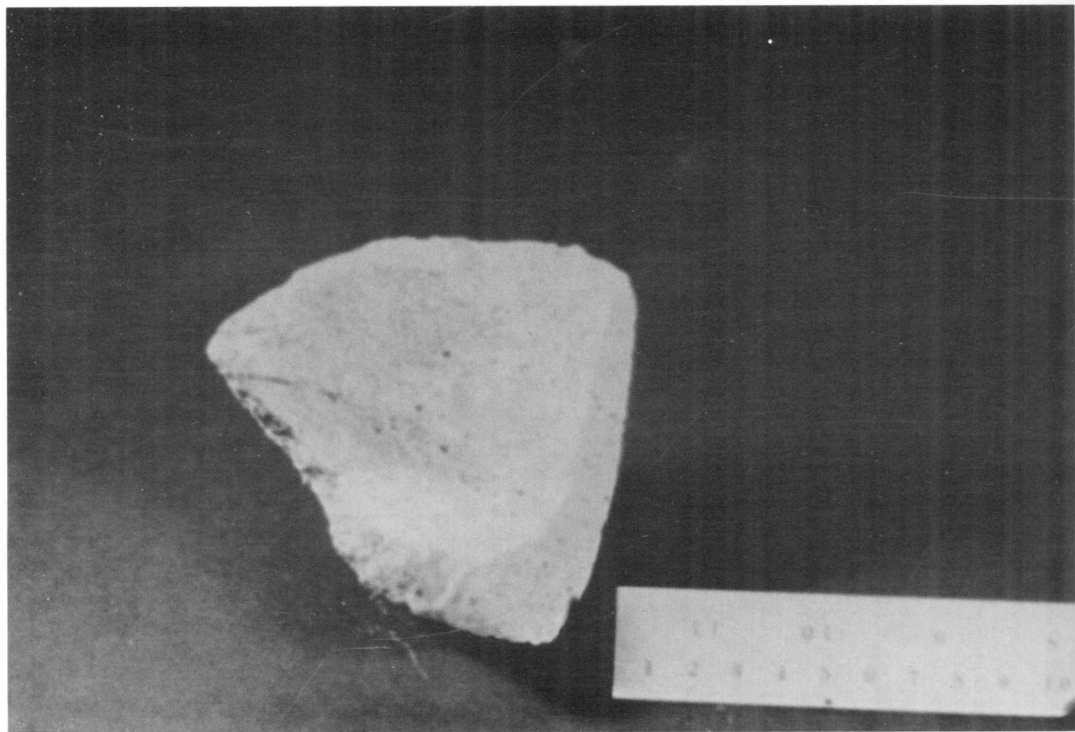


Fig. 15. Fragment of a pre-pottery Neolithic gypsum bowl from Abu Hureyra, Syria, ca. 6500 B.C.

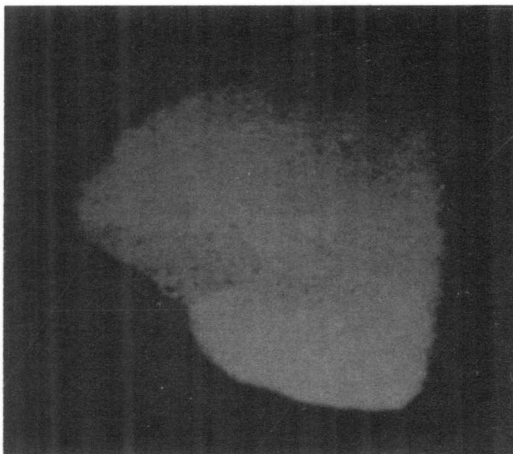


Fig. 16. Abu Hureyra gypsum bowl (Fig. 4). Contact (no magnification) x-ray image obtained with industrial x-ray film

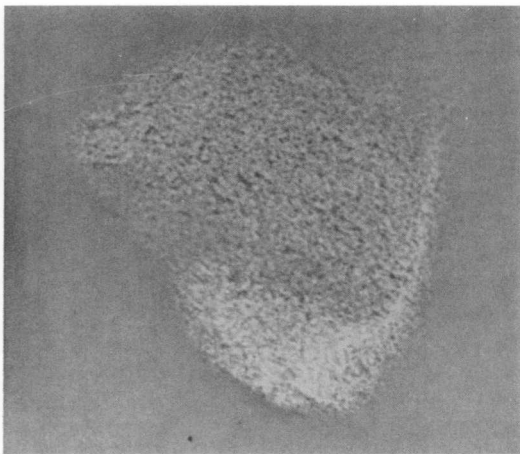


Fig. 17. Abu Hureyra gypsum bowl (Fig. 4). Image obtained by using a Xerox 126 imaging plate as the x-ray image receptor

resolution limit (50 microns) of these images, or the expected porosity has been altered by setting and weathering.

Joints in archaeological plasters such as the Pre-pottery Neolithic bowl from Abu Hureyra have been particularly difficult to image by radiographic techniques, probably because of the acicular crystal growth during setting and Ostwald ripening during aging, and because of the large volume fraction (up to 60 percent) of well-dispersed, fine porosity. A few pores are large (up to 3 mm.), but most are fine (0.001 to 0.05 mm.). Some barely visible black flecks of elongated charcoal remaining from the initial process of burning the gypsum are dispersed in the matrix but appear as angular pores in radiographs. Because it has a low density, the charcoal can be differentiated from pores in the radiographs only by shape. In other instances, we have found calcium-containing layers accreted on the surfaces of pottery vessels which obscure the pottery structure beneath—sometimes because of high-density calcium-containing phases such as apatite, aragonite, and anhydrite, and sometimes because of decreased penetration due to the increase in thickness.

DISCUSSION

Aspects of structural details which bear on the choice of imaging methods are their size, density of materials relative to background matrix, and their distribution, lo-

cation, and orientation within the object—features which are sometimes mutually exclusive. The size of a characteristic detail puts limits on the required spatial resolution and differs with each instrument (Table 2). In general, the attenuation coefficient of x-rays (essentially the limit of penetration) for the sample is proportional to the average density and can be summed across a wall thickness (Table 1).

The exposure time and x-ray energy (x-ray source current, and especially x-ray voltage) are best calculated by taking into

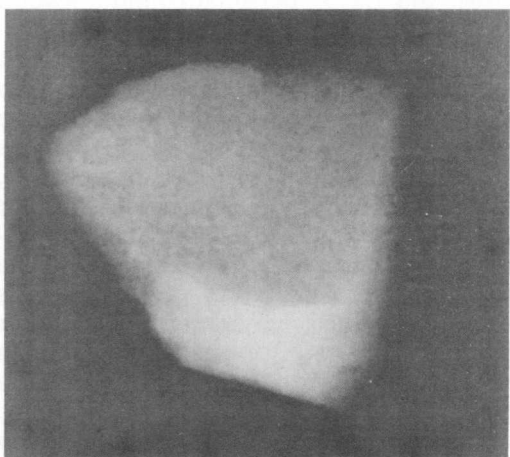


Fig. 18. Abu Hureyra gypsum bowl (Fig. 4). Image obtained by using a photostimulable phosphor plate as the x-ray image receptor

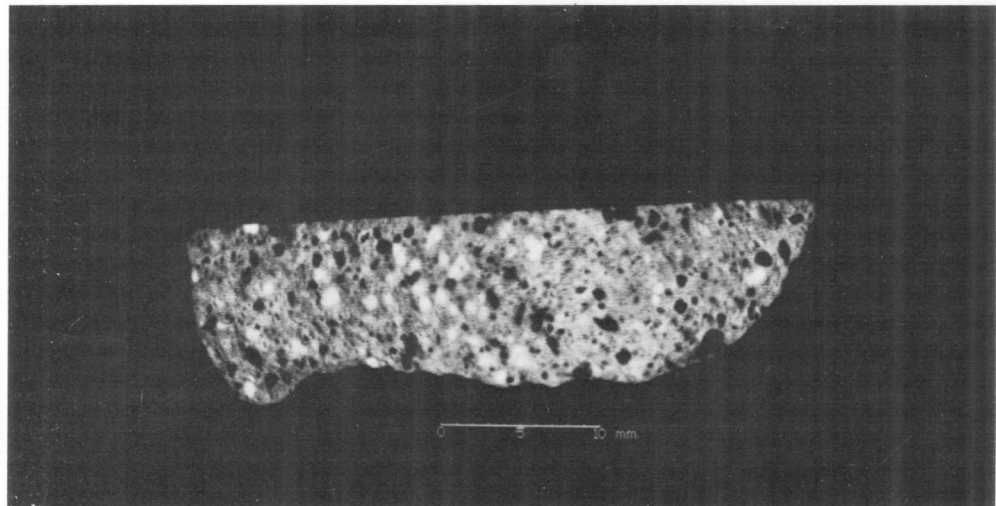


Fig. 19. Abu Hureyra gypsum bowl. Micro-CT image of a part of a thick-section slice. High density inclusions are white, and pores are black.

account object and feature sizes, x-ray source spectrum, energy dependences of the materials' x-ray attenuation coefficients, and the efficiency of the detector (for CT parameter optimization, see Séguin and Bjorkholm 1988).

Various processes have peculiarities which must be taken into consideration. In the Xerox 126 process, positive images optimize porosity (Fig. 4b), but negative images better display details of mineral inclusions (Fig. 4c). Distinctly different information is derived from the two modes (Reginald Davis, personal communication 1987).

Inclusions can usually be imaged without special procedures when they differ from the clay matrix by about 10 percent relative specific gravity, if they are larger than the spatial resolution limit of the technique, and if the maximum diameter is a major fraction of the wall thickness (the last condition is not necessary for CT imaging). The location and orientation of such details within the object may determine whether a projection or CT image is required. In projection systems the orientation of the object is critical.

Information about ceramic fabrication techniques can be maximized by imaging a single-wall thickness, thereby eliminating the problem of distinguishing information

from double-wall thicknesses where the structural information from each wall is superimposed, leading to confusion. For this reason, bowls or large fragments are more easily imaged than closed-mouth vessels. Joint interfaces usually will be clearly imaged only if they are parallel to the viewing direction. Even though the quality of the image may suffer, film radiography and photostimulable phosphors are sometimes preferable because the film or phosphor receptor can be bent into convenient shapes, a maneuver which is impossible with Xerox cassettes or solid-state detector arrays. Film and electrostatic and photostimulable phosphor receivers allow images to be magnified three to five times by elevating the sample above the receiver, but some distortion and loss of resolution are incurred owing to parallax. In addition, spatial resolution can be modified by changing the size of the x-ray source spot and the relative positions of source, object, and detector.

Because cracks are more likely to form due to differential drying, joints in high-shrinkage earthenware tend to be more prominent than those in low-shrinkage stonewares. An additional factor in imaging high temperature ceramics is that the amount of glassy phase is greater than in earthenware, so the pores are somewhat rounded and densification lessens the

amount of porosity. The effects of the glassy phase combined with the fine size of pores make overfired earthenware, stoneware, and porcelain much more difficult to image, unless the bodies have bloated and warped, producing porosity not related to forming. One advantage of the greater vitrification and lower porosity in most fine porcelains and vitreous stonewares is that subtle variations in wall thickness can be imaged without interference from pores and inclusions.

Gypsum plasters are difficult to image because of the distribution of pores and solid phase. In one example, the same total volumetric quantity of pores was found in a gypsum plaster as in fired earthenware, yet structural details were imaged in the earthenware but not the plaster. Examination of fractured and polished cross sections with a scanning electron microscope showed that in the plasters most of the porosity and the solid phase were concentrated in fine features which were below or near the effective resolution limit of many imaging methods (averaging 0.25–5.0 microns with a range of 0.1–3000 microns); thus, structural features are present in images as noise or lost. In contrast, the extent of solid phase in earthenware was greater than that of the pores and greater than the resolution of most imaging methods, averaging on the order of 50 to 100 microns, with a range of 1 to 10,000 microns.

SECONDARY IMAGE PROCESSING AND PUBLICATION

Once the structural features of interest have been imaged using the proper techniques, the final problem is one of documentation, which involves image display, publication, and storage. Many radiographic images of the complex and detailed structures of ceramics which appear in publications are poor because of the difficulty of transferring an image from one medium to another, that is, from the actual x-ray image as it is viewed in its original medium to the printed page. For instance, printed images have limited contrast and poor resolution compared to the radiographic techniques described here. Often images are reduced in size, further limiting resolution. This problem may be solved when distri-

bution of images through computer networks becomes common and the resolution of computer-generated hard copy increases. Until then, the poor quality of published radiographs probably will continue to limit the application of radiography to ceramics. Secondary processing methods, however, can be used to enhance images for publication so that essential structural features will be reproduced on the printed page.

The most inexpensive and simple options involve the printing of multiple images. One approach which works particularly well with x-ray film images is to use several exposure times from a single x-ray film to highlight areas of different density in the film. Each exposure should be taken directly from the original film, because every intermediate printing step from original to publication cuts final resolution by about 20 percent. Because narrow dynamic range is coupled with high contrast in x-ray film, a printed film image will contain areas which are over- and under-exposed and many details will appear murky (e.g., Fig. 13). Another approach, particularly useful with xeroradiography, is to take a series of different images with imaging parameters chosen to optimize particular features, such as wall contour, inclusions, or pores, and then publish multiple images of one vessel or sherd. Published images may also be enhanced by image intensifiers and filters, but neither technique was included in this study.

More sophisticated options involve the enhancement of images with digital image processing (e.g., Figs. 1–3; see also Séguin 1991). Image processing programs abound and their uses have recently undergone a rapid proliferation from the early programs used for photogrammetry and micrography (Druzik et al. 1982a; 1982b; Estes, Jensen, and Tinney 1977; Frischein 1982; Ogleby and Rivett 1985; Scollar 1983; Scollar and Weidner 1981; Thompson and Stanforth 1982; Van Schoute and Verougstraete-Marcq 1986). Using image processing, it is possible to select particular features for emphasis.

Digital image processing can be performed only on images which are in digital form. X-ray film images can be successfully converted to digital format, while xerora-

diographs are more difficult, but Robert Johnston of the Rochester Institute of Technology announced at the Third International Symposium on Ancient Ceramics (Shanghai, November 1989) that he has now succeeded in converting the latter. Previously, Davidson and Vandiver were unsuccessful in digitizing xeroradiographs made with the Xerox 126 process because the bright edges, used to detect structural features, are obscured by concentric alternating dark and light halos which form around them. Without image processing, the blue Xerox 126 images reproduce only as low-contrast photographs, even though the blue original is easier for most people to interpret than the black (Xerox 175) one. The Xerox 175 process reproduces as a high-contrast image, but only limited success has been achieved in digitizing images made with these plates because of the halo problem.

Images from the more recent imaging systems which provide raw data in digital form, such as photostimulable phosphor receptors, CT-scanners, and digital projection systems, are natural candidates for extensive enhancement through selective filtering, transformations, and other operations. A thick section of a plaster bowl from Abu Hureyra was imaged with the high-resolution, digital projection radiography system (Fig. 1). The image was inspected on a video monitor with adjustable gray-scale mapping, and then subjected to image processing manipulations designed to highlight different structures. High-pass filtering in frequency space suppresses that part of the dynamic range of the image corresponding to the overall structure and brings out small-scale structure more clearly in all parts of the image simultaneously (Fig. 2). The result is a type of edge enhancement not unlike that seen in xeroradiographic images. Another type of edge enhancement (Fig. 3) results from calculating a directional gradient of pixel values in the original image. In these edge-enhanced versions of production images, much of the visible structure is actually due to the irregular texture of one of the rough surfaces of the sample rather than to the internal structure, because every projection

image superposes structures in all planes that lie perpendicular to the viewing direction. (This is one of the reasons for the importance of CT images, which do not suffer from superposition problems.) As these figures demonstrate, the visibility of features can be greatly affected by manipulation of the image.

The resolution of direct digital radiography is still limited to about 50 microns, and processing of images is often time-consuming. If a structural feature cannot be seen or directly imaged, extensive processing is a gamble, and if other means of low-tech visualization are possible, it may be redundant. By combining radiography with scanning electron microscopy (SEM), it is possible to determine the range of structural details in a whole object and, thus, whether a microscopic sample of an artifact is representative of the whole. Similar information is gained at greater magnification but without the range and extent of heterogeneity possible with radiography. SEM in backscattered mode shows atomic number contrast and in secondary electron imaging mode the structural detail of pores and inclusions.

CONCLUSIONS

Three areas of x-ray imaging technology are the focus of current research in medical, materials, and museum research: (1) development and optimization of x-ray sources and investigation of alternative ones, (2) development of receivers for specialized applications, and (3) secondary processing for visualization and interpretation, storage, or publication.

The structural integrity and fabrication of ceramic materials can be assessed using such criteria as porosity, internal cracks and joins, and surface flaws. Because of its spatial resolution of 2 to 5 microns, ordinary high-resolution film radiography is a better non-destructive evaluation (NDE) imaging method than xeroradiography, photostimulable phosphors, or other techniques for the determination of the shape, size, and distribution of surface-impairing and internal flaws which lead to brittle fracture in advanced structural ceramics (Ellingson 1988). However, film radiography is limited

by low dynamic range. In determining the methods of manufacture of modern and ancient pottery and plasters, xeroradiography with Xerox 126 equipment offers advantages of both positive and negative images, and the enhancement of edges, internal joints, and boundaries between pore and solid phase or clay matrix and inclusions, primarily because of the larger dynamic range of the plates and the features inherent in electrostatic imaging. The Xerox 175 system, which no longer is on the market, cannot produce positive images, but this disadvantage is offset by its ability to obtain high contrast, higher spatial resolution images. The black particles of the Xerox 175 system measure about 10 microns, about half the size of those used in the earlier 126 process, with an attendant increase in resolution by a factor of 2. The disadvantages of the Xerox 126 blue-and-white images are poor contrast for reproduction in publications and somewhat coarse resolution. The edge enhancement and multiple halos do not allow straightforward digitization for image processing, but the ease and speed of the process are a compensating factors.

Photostimulable phosphors, direct digital radiography, and high-resolution CT all have spatial resolutions that do not yet match those of film or xeroradiography, but the advantages of superior dynamic range and digital processing options can make them very useful. Computed tomography always offers the great advantage that it shows internal structure directly, without the superposed structures that complicate the interpretation of projection radiographs made with film or any other medium. It provides the only possibility for visualizing and quantifying pores and inclusions inside objects which have complicated structures.

The researcher can now choose from a range of x-ray imaging methods. Many are not readily available, but future developments should improve their accessibility and performance. For particular imaging problems, the best instruments, operating parameters, and secondary processing have to be determined by balancing the requirements of the project with instrument characteristics.

Acknowledgments

We thank Fance Franck, Paris; Mary Voigt, College of William and Mary; and Andrew Moore, Yale University, for samples and much useful discussion. We are most grateful to Betty Seed and Louise Corkham of Cambridge City Hospital, Cambridge, Massachusetts; Dr. Terrence Connor and Elizabeth Allen of Women's College Hospital, Toronto, for their help with radiography. Tom Davidson is thanked for helping to digitize xeroradiographs and Harold Dougherty for printing the film radiographs.

REFERENCES

- Alexander, Robert E. and R. H. Johnston
1982 Xeroradiography of Ancient Objects: A New Imaging Modality. In *Archaeological Ceramics*, edited by Jacqueline S. Olin and Alan D. Franklin, pp. 145-154. Smithsonian Institution Press, Washington, D.C.
- Boag, J. W.
1975 New Ways with X-rays: Xeroradiography and Ionography. *Physics in Technology* 6.5: 209-216.
- Bokman, W.
1982 Xeroradiography in Conservation. *Abstracts. I.I.C. Ninth International Congress on Science and Technology in the Service of Conservation*, p. 1. Washington, D.C., 3-9 September 1982.
- Bourriau, Janine
1985 Technology and Typology of Egyptian Ceramics. In *Ancient Technology to Modern Science, Ceramics and Civilization*, Vol. I, edited by W. D. Kingery, pp. 27-42. American Ceramics Society, Columbus, Ohio.
- Braun, David P.
1982 Radiographic Analysis of Temper in Ceramic Vessels: Goals and Initial Methods. *Journal of Field Archaeology*. 9.2: 183-192.
- Cort, Louise A.
1979 *Shigaraki, Potters' Valley*. Kodansha, Tokyo.
- Digby, A.
1948 Radiographic Examination of Peruvian Pottery Techniques. *Actes du XXVIII Congrès International des Américainistes*. Paris.
- Druzik, James R., D. Glackin, D. Lynn, and R. Quiros
1982a Applications of Computer-based Image Processing Useful in Conservation. *Preprints. 10th Annual Meeting, American Institute for Conservation*, pp. 71-72. Milwaukee, May 1982.
- 1982b The Use of Digital Image Processing to Clar-

- ify the Radiography of Underpainting. *Journal of the American Institute for Conservation* 22: 49–56.
- Ellingson, William A.**
- 1988 Recent Developments in Nondestructive Evaluation for Structural Ceramics. Argonne National Laboratory Report ANL-87-53. Argonne, Illinois (1987).
 - Ellingson, William A., Pamela B. Vandiver, T. K. Robinson, and J. J. Lobick
 - 1988 Radiographic Imaging Technologies for Archaeological Ceramics. In *Materials Issues in Art and Archaeology*, edited by E. V. Sayre, Pamela B. Vandiver, James R. Druzik, and C. Stevenson, pp. 25–32. Proceedings of the Materials Research Society, Vol. 123. Materials Research Society, Pittsburgh.
 - Estes, J. E., J. R. Jensen, and L. R. Tinney**
 - 1977 Use of Historical Photography for Mapping Archaeological Sites. *Journal of Field Archaeology* 4: 441–447.
 - Foster, Giraud V.**
 - 1985 Identification of Inclusions in Ceramic Artifacts by Xeroradiography. *Journal of Field Archaeology* 12: 373–376.
 - Frischein, W.**
 - 1982 Computer Enhancement of Radiographic Films Used in Structural Investigation of an Historic Structure. *Bulletin of the Association for Preservation Technology* 14.2: 18–25.
 - Glanzman, William D.**
 - 1983 Xeroradiographic Examination of Pottery Manufacturing Techniques: A Test Case from the Baq'ah Valley, Jordan. *MASCA Journal* 2.6: 163–169.
 - Glanzman, William D. and Stuart J. Fleming
 - 1985 Ceramic Technology at Prehistoric Ban Chiang, Thailand: Fabrication Methods. *MASCA Journal* 3.4: 114–121.
 - 1986 Xeroradiography: A Key to the Nature of Technological Change in Ancient Ceramic Production. *Nuclear Instruments and Methods in Physics Research* A242: 588–595.
 - Gourdin, William H. and W. David Kingery**
 - 1975 The Beginnings of Pyrotechnology: Neolithic and Egyptian Lime Plaster. *Journal of Field Archaeology* 2: 133–150.
 - Henrickson, Robert**
 - 1991 Wheelmade or Wheel-finished? Interpretation of 'Wheelmarks' on Pottery. In *Materials Issues in Art and Archaeology II*, edited by Pamela Vandiver, James Druzik and George S. Wheeler, pp. 523–542. Proceedings of the Materials Research Society, Vol. 185. Materials Research Society, Pittsburgh, Pennsylvania.
 - Heinemann, S.**
 - 1975 Xeroradiography: A New Archaeological Tool. *American Antiquity* 41.1: 106–111.
 - Kaneko, Hiroyuki, Tsugio Matuzawa, and Makoto Sahara
 - 1989 *Report of the Yamanouchi Sugao Archaeological Collection*. No. 1. Nara National Cultural Properties Research Institute, Nara, Japan.
 - Kao, M., A. Chung-Bin, J. Lobick, and S. Balter**
 - 1987 Using Computed Radiographic Systems for Electron Beam Portal Films. American Association of Physicists in Medicine, Annual Meeting, Chicago, 1987.
 - Kingery, W. David and Pamela B. Vandiver**
 - 1986 *Ceramic Masterpieces: Art, Structure, and Technology*. Macmillan Free Press, New York.
 - Kingery, W. David, Pamela B. Vandiver, and M. Prickett
 - 1988 The Beginnings of Pyrotechnology, Part II: Production and Use of Lime and Gypsum Plaster in the Pre-Pottery Neolithic Near East. *Journal of Field Archaeology* 15: 219–244.
 - Koyama, Fujio**
 - 1973 *The Heritage of Japanese Ceramics*. Weatherhill, New York.
 - Kureya, M., S. Miura, A. Osaki, and T. Kaneko**
 - 1983 Conditions for Obtaining Density Characteristics of X-ray Film Corresponding to Various Thicknesses of Bronze and Japanese Cypress. *Scientific Papers on Japanese Antiques and Art Crafts* 28: 28–37.
 - Magliano, P. and B. Boesmi**
 - 1988 Xeroradiography for Paintings on Canvas and Wood. *Studies in Conservation* 33.1: 41–47.
 - Mix, P. E.**
 - 1987 *Introduction to Nondestructive Testing*. John Wiley and Sons, New York.
 - Moore, Andrew M. T.**
 - In preparation *Abu Hureyra*. Yale University Press, New Haven.
 - Nakayama, H.**
 - 1953 Experiments on X-ray Penetration on Japanese Pigments. *Bijutsu Kenkyu* 168: 127–130.
 - Ogleby, C. and L. J. Rivett
 - 1985 *Handbook of Heritage Photogrammetry*. Australian Heritage Commission Special Publication No. 4. Sydney, Australia.
 - Peterson, Susan H.**
 - 1974 *Shoji Hamada: A Potter's Way and Work*. Kodansha International, Tokyo.
 - 1977 *The Living Tradition of Maria Martinez*. Kodansha International, Tokyo.
 - 1984 *Lucy M. Lewis: American Indian Potter*. Kodansha International, Tokyo.
 - Rice, Prudence**
 - 1987 *Pottery Analysis: A Sourcebook*. University of Chicago Press, Chicago.
 - Rye, Owen S.**
 - 1977 Pottery Manufacturing Techniques: X-Ray Studies. *Archaeometry* 19.2: 205–211.
 - Scollar, Irwin**
 - 1983 Digital Image Processing and Archaeological Air Photography. In *Proceedings of the Seminar, Mohenjo-daro Research Project: Documentation in Archaeology, Techniques, Methods, Analyses, December, 1981*, pp. 137–142. Aachen.

- Scollar, Irwin and B. Weidner
 1981 Computer Restitution and Enhancement of Extreme Oblique Archaeological Air Photos for Archaeological Cartography. *Revue d'Archéométrie* 2.5: 71–80.
- Séguin, Fredrick H.
 1991 High-Resolution Computed Tomography and Digital Radiography for Archaeological and Art-Historical Objects. In *Materials Issues in Art and Archaeology II*, edited by Pamela Vandiver, James Druzik, and George S. Wheeler, pp. 65–72. Proceedings of the Materials Research Society, Vol. 185. Materials Research Society, Pittsburgh, Pennsylvania.
- Séguin, Fredrick H. and P. J. Bjorkholm
 1988 Optimization of Parameters for High-Resolution X-Ray Computed Tomography. In *Review of Progress in Quantitative NDE*, Vol. 8, edited by D.O. Thompson and D.E. Chimenti, pp. 275–280. Plenum Press, New York.
- Séguin, F. H., P. Burstein, P. J. Bjorkholm, F. Homburger, and R. A. Adams
 1985 X-Ray Computed Tomography with 50-micron Resolution. *Applied Optics* 24: 4117–4123.
- Sonoda, Minoru, Masao Takano, Junji Miyahara, and Hisatoyo Kato
 1983 Computed Radiography Utilizing Scanning Laser Stimulated Luminescence. *Radiology* 148: 833 ff.
- Takahashi, K., K. Kohda, and J. Miyaha
 1984 Mechanisms of Photostimulated Luminescence in BAFX Eu₂m+(X=Cl,Br) Phosphors. *Journal of Luminescence* 31/32: 226 ff.
- Thompson, Gary and S. Stanforth
 1982 Identification and Measurement of Change in Appearance by Image Processing. In *Science and Technology in the Service of Conservation*, pp. 159–161. International Institute for Conservation, Conference Preprints.
- Thourson, T. L.
 1975 Xeroradiography. *Journal of the Society of Photo and Optical Instrumentation and Engineering* 56: 225–235.
- Todd, H. N. and R. D. Zakia
 1969 *Photographic Sensitometry: The Study of Tone Reproduction*. Morgan and Morgan, New York.
- van As, Abraham
 1984 Reconstructing the Potter's Craft. In *The Many Dimensions of Pottery: Ceramics in Archaeology and Anthropology*, edited by S. E. van der Leeuw and A. C. Pritchard, pp. 130–159. University of Amsterdam, Amsterdam.
- Van Schoote, R. and H. Verougstraete-Marcq
 1986 Radiography. *PACT* 13: 131–157.
- Vandiver, Pamela B.
 1985 Sequential Slab Construction: A Near Eastern Pottery Production Technology, 8000–3000 B.C. Ph.D. dissertation, Department of Materials Science and Engineering, Massachusetts Institute of Technology.
 1987 Sequential Slab Construction: A Conservative Southwest Asiatic Tradition ca. 7000–3000 B.C. *Paléorient* 13.2: 9–36.
 1988 The Implications of Variation in Ceramic Technology: The Forming of Neolithic Storage Vessels in China and the Near East. *Archaeomaterials* 2: 139–174.
 in press Ceramic Technology at Mehrgarh. In *Mehrgarh: The Neolithic Period*, edited by J.-F. Jarrige and R. Meadow.
- Vandiver, P. B. and C. G. Koehler
 1986 Structure, Processing, Properties and Style of Corinthian Transport Amphoras. In *Technology and Style, Ceramics and Civilization*, Vol. II, edited by W. David Kingery, pp. 173–216. American Ceramics Society, Columbus, Ohio.
- Vandiver, P. B. and P. Lacovara
 1985–86 An Outline of Technological Changes in Egyptian Pottery Manufacture. *Bulletin of the Egyptological Seminar* 7: 53–86.
- Voigt, Mary
 1983 *Hajji Firuz Tepe, Iran: The Neolithic Settlement*. University Museum, University of Pennsylvania, Philadelphia.
- Wolfe, J. N.
 1973 Xeroradiography: Image Content and Comparison with Film Roentgenograms. *American Journal of Roentgenology* 117.3: 690–695.
- Young, Jr., T. Cuyler, and L. D. Levine
 1974 *Excavations of the Godin Project: Second Progress Report*. Art and Archaeology Occasional Paper 26. Royal Ontario Museum, Toronto, Canada.